

1 **Electrical properties speculation of contamination by water and gasoline on sand**
2 **and clay composite**

3 Mohamed M. Gomaa¹ and Mohamed Elnasharty², Enzo Rizo³

4 ¹ National Research Centre, Geophysical Sciences Dept., Cairo, Egypt. Email:

5 mmmmsgomaa@yahoo.com, Fax: 00233370931

6 ² Microwave Physics and Dielectrics Dept., Physics Division, National

7 Research Centre, Dokki, Giza, 12622, Egypt

8 ³ National Research Council (CNR-IMAA), CNR-IMAA, Hydrogeosite

9 Laboratory, Polo di Marsico Nuovo, c.da Fontanelle - 85052 Marsico Nuovo

10 (PZ) – Italy.

11 **ABSTRACT**

12 Effects of temperature, frequency, and molarity on electrical conductivity
13 have been studied for sand-clay samples contaminated by water and gasoline.
14 Electrical properties changes according to frequency, contaminant type and
15 structure of components at the sample. A comparison was performed for these
16 contaminated sand-clay samples. Changes of dielectric constant (ϵ'),
17 conductivity (σ) and complex impedance with frequency (0.1 Hz $2 \times 10^7 \text{ Hz}$),
18 with different contaminant concentration (at constant room temperature $\sim 21^\circ\text{C}$)
19 have been studied. The sand-clay samples were mutually wetted gradually
20 using gasoline and distilled water. Then, electrical properties were measured
21 sequentially. Water is a conductive liquid and the contaminant gasoline is an
22 insulator. The experimental results indicate that, conductivity of samples
23 increases with increase of water concentration while with the additions of the

24 contaminant gasoline, the sample conductivity decreases. The permittivity,
25 decreases with reduction of conductive links between grains and with the
26 progressive increase of frequency. The conduction of electrical conductivity,
27 commonly, increases with increase of connectivity between different links
28 between grains. Also, conduction increases with progressive increase of
29 frequency. Comparison of both outcomes from lab electrical measurements
30 gives a speculation about the picture in the field.

31 **Keywords:** Electrical properties; conductivity; water saturation; gasoline
32 saturation; permittivity; frequency.

33 INTRODUCTION

34 There are many physical, chemical and mechanical properties that can
35 affect the electrical properties. These parameters may be grain shape, size,
36 orientations, interface boundaries, porosity, inhomogeneity, combination made
37 by mixing substances together, and structural interconnected pores of the
38 conducting and insulating fractions of the grains ... etc. Also, wetting the
39 samples with liquid is an efficient factor for the changing of electrical
40 characteristics (Gomaa and Abou El-Anwar 2015). The systematic
41 investigation of ac conductivity at various temperatures and frequencies gives
42 valuable information on conduction mechanisms at samples according to its
43 electric charge carriers (Gomaa 2013). In general, the gradual additions of
44 conductor concentration raise the conductivity value (Abou El-Anwar and
45 Gomaa 2016). Also, the gradual additions of conductor concentration decrease
46 the distance spaces separating two grains and, accordingly, raises the

47 permittivity values (Gomaa and Elsayed 2009). The latter increase of
48 conductivity and permittivity is present until the samples reach the percolation
49 concentration threshold (Gomaa 2008). Percolation threshold of concentration
50 is the conductor concentration fraction that permits complete contact between
51 electrodes.

52 Increase of conductivity is the outcome of growing of uninterrupted
53 conduction links of conducting elements (water). The conduction values of
54 conductivity are faint at relatively low overall conductor amount. With
55 progressive increase of overall conductor amount the conductivity becomes
56 greater (Gomaa et al. 2018, Gomaa and Kassab 2017). Generally, with increase
57 of overall conductor amount and with progressive increase of frequency more
58 continuous conductor links start to be established between the different grains
59 (Gomaa et al., 2009). Increase of continuous conductor links leads to the
60 general increase of conductivity values (Knight and Endres 1990). The raise of
61 frequency initiates particles to overcome energy barriers between atoms and
62 therefore the conductivity value is increased. The growing of frequency makes
63 the permittivity decreases. Also, decrease of permittivity is initiated from
64 decrease of conductor concentration. When the conductor concentration
65 decreases, this leads, generally, to increase of insulator material along the
66 space separating the conducting grains. Permittivity values increase with
67 increase of total conductor concentration until it achieves the dispersion limit.
68 At that limit, the permittivity may decrease again above that percolation limit
69 (Gomaa and Alikaj 2009, Gomaa and Abou El-Anwar 2017). The small pores

70 among grains result in relative decrease of permittivity in samples
71 (Barabanova et al. 2013). Permittivity changes from one specimen to another
72 due to alteration of combinations, volumes and amounts of the conducting and
73 insulating materials in specimen. Also, there may be the texture between grains
74 (Gomaa et al., 2015 a and b). Conductivity, in general, has a monotonic
75 attitude of increase with the successive increase of frequency. The permittivity,
76 in general, has a tendency to increase with decrease of the frequency (Kassab
77 et al. 2017, Gomaa 2006).

78 Frequency behavior of conductivity is may resulted from orientation and
79 translational hopping mechanisms. Orientation mechanism means hopping and
80 jumping of electron in the space separating two charged defects. The
81 translation hopping means that there is D C conductivity at zero frequency.
82 Imaginary impedance, which depends on frequency, point to the existence of
83 different reactions in the system.

84 Comparing effect of water as a conductor and that of gasoline as an
85 insulator, with both frequency and wetting at lab was done in this work. To
86 achieve this study, a sand-clay sample was measured (electrically) at
87 laboratory. The samples was measured dry and at different contamination
88 saturations, of water and gasoline, at constant room temperature (~21 °C), at
89 frequency range of (0.1 Hz up 2×10^7 Hz). Electrical measurements;
90 permittivity, conductivity and complex impedance compared to frequency,
91 declare effect of contaminants and texture on the studied samples. The water is
92 conductive liquid, because miscibility of salts found in its structure and the

93 gasoline is insulator (Abou El-Anwar and Gomaa 2013). In the laboratory,
94 conductivity of samples increases with sample's water content while with
95 additions of gasoline the sample conductivity decreases. Wetting the samples
96 with liquid is effective factor in the change of electrical responses (Gomaa and
97 Kassab M., 2016).

98 In the current paper we will compare both outcomes from electrical
99 measurements from different contaminants (water and gasoline) and we will
100 discuss wetting conditions of water, gasoline and frequency on electrical
101 laboratory measurements.

102 **Experimental Details**

103 **Electrical measurements**

104 Dielectric was measured using broadband dielectric spectrometer concept,
105 Novo Control, Germany, at wide frequency range (0.1 Hz $2 \times 10^7 \text{ Hz}$). We
106 apply testing voltage of 1 Vrms at constant room temperature ($\sim 21 \text{ }^\circ\text{C}$). Sample
107 constituents are some small sand grains that are naturally mixed with some clay
108 impurities. The disc shaped sample holder has dimensions of 8 mm diameter
109 and 3.623 mm height with total volume of 0.182 cm^3 . Data were automatically
110 measured and studied by the instrument software WinDeta. The sample was
111 enclosed between two copper electrodes and a Teflon cylinder. The sample
112 then placed in its proper position inside the instrument. Measurements were
113 done in a row, pure sand-clay mixture and then $10 \text{ }\mu\text{L}$ of filtered water or
114 gasoline was added to sample and measurement repeated. The last step was
115 repeated until the water volume in the specimen reaches $60 \text{ }\mu\text{L}$ of filtered

116 water. The sample sand cell is present at Fig. (1), 1: is the Teflon cylinder and
117 2: indicates the two copper electrodes. Dielectric constant was calculated by the
118 formula $\epsilon' = \frac{C_p d}{\epsilon_0 A}$ (Jonscher 1973, 1975, 1977 and 1999, Hill and Jonscher
119 1983). The ac conductivity is given by $\sigma = w \epsilon' \epsilon_0$ (Hill and Jonscher 1983),
120 where w is the angular frequency.

121

122 **Results and Discussion**

123 Electrical properties of any mixture of samples are affected by:

124 1- The change of sample arrangement during pumping of the water or
125 gasoline. This may render inaccurate measurements as the field sample has
126 changed in its structure. This gives misleading data. Consequently, it would be
127 better to remove washout of the measured samples.

128 2- Using samples of large volume is suitable for electrical field
129 measurements. However, this may contradict the condition for laboratory
130 electrical measurements which is instituted on using of small volumes with
131 large areas. Physically, the laboratory sample must have small thickness to
132 form electric field with proper strength to minimize errors.

133 **1) Chemical assembly of gasoline**

134 Gasoline is a reiterated component of a liquid mixture of hydrocarbons. It
135 is consisted of mixtures of hydrocarbons, blending agents, and additives.
136 Commonly, the chemical constituents of gasoline hydrocarbons changes
137 extensively (IARC 1989). This dependence is affected by crude oils
138 concentrations, the filter procedure used, and the product precise requirement.

139 The gasoline composition range from 6 to 13 % of alkanes; 25 to 40 % iso-
 140 alkanes; 3 to 7 % cyclo-alkanes; 1 to 4 % cyclo-alkenes; and from 20 to 50 % of
 141 overall aromatics (0.5-2.5% benzene). Detailed information regarding the
 142 Chemical analysis, particle size analysis, hydrogeological properties are located
 143 at Table (1). The sand used is identified by the properties at Table (1).

144

Table 1 - Chemical analysis, Particle size analysis, Hydrogeological properties

Chemical analysis results										
	SiO ₂	TiO ₂	Al ₂ O ₃	MnO	Fe ₂ O ₃	MgO	CaO	Na ₂ O	K ₂ O	CO ₂
%	81.17	0.06	4.75	0.05	0.56	0.13	6.67	0.83	1.15	4.02
Particle size analysis of sand										
d (mm)	0 - 0.074	0.075 - 0.104	0.105 - 0.149	0.150 - 0.420	0.421 - 0.840	0.841 - 2.000	>2.001			
%	0.8	0.03	0.20	14.27	70.67	10.6	3.43			
Hydrogeological properties										
d (mm)	K _{max} (m/s)			ρ (%)						
0.09	5*10 ⁻³			35						

145

146 2) Laboratory electrical measurements

147 Figure (2) shows the series resistance (R_s) with frequency spectrum and
 148 distinct concentrations of filtered water (10 μL, 20 μL, 30 μL, 40 μL, 50 μL
 149 and 60 μL). The dry sand-clay samples have the highest resistance (Song et al.
 150 1986, Leroy et al., 2008, Chew and Sen 1982, Chelidze and Guéguen 1999).

151 With the consecutive changes of distilled water, the resistance decreases. Series
 152 resistance steps down when adding the 1st and 2nd successive additions of
 153 distilled water. The decrease is slowly with the 3rd, 4th and 5th successive
 154 additions. The last successive addition, 6th dose, had a mild decrement reaching

155 minimum values of series resistance for sand-clay composite (e. g. Chelidze et
156 al. 1999, Sen 1984, Sen 1981, Olhoeft 1977). This is nearly the full saturation
157 of sand-clay sample. The sample series resistance descended three decades
158 with successive additions from dry to full saturation (Shaltout et al, 2012,
159 Gomaa 2009). When specimen is dry (0 μL), decrease of the resistance value
160 with frequency is fast and requires nearly more than one decade for the whole
161 frequency range (Olhoeft 1976, Olhoeft 1980, Olhoeft 1985). When specimen
162 is wetted with the other successive additions of water (10 μL , 20 μL , 30 μL , 40
163 μL , 50 μL and 60 μL), decrease of the resistance with frequency is slow and
164 takes nearly half decade in the whole frequency range (Minaw et al. 1972,
165 Levitskaya and Sternberg 1996 a, b, Levitskaya 1984).

166 The dry sample does not reach saturated (flat) resistance value, even at
167 very high frequency (2×10^7 Hz), while the other wet samples (10 μL , 20 μL ,
168 30 μL , 40 μL , 50 μL and 60 μL) reaches the saturated (flat) resistance value at
169 relatively lower frequencies (10^3 Hz), and differs gradually from one saturation
170 to the other (Gomaa and Elsayed 2006, Gomaa et al. 2000). As the saturation
171 concentration increases, the saturated (flat) resistance value at definite
172 frequency is decreased (Mendelson and Cohen 1982, Last and Thouless 1971,
173 Knight and Nur 1987). The sample series resistance nearly takes three decades
174 from the dry condition to the full saturation in the whole frequency range.

175 Figure (3) displays the series resistance (R_s) with frequency dry and at
176 various saturations of gasoline. The dry sand-clay samples have the lowest
177 resistance. Series resistance (R_s) increases with adding gasoline concentrations

178 (10 μL , 20 μL , 30 μL , 40 μL , 50 μL and 60 μL).. Subsequent gasoline additions
179 are quite different from water additives. The series resistance is directly related
180 to gasoline addition. However, the whole of growth of the series resistance was
181 within one decade at the whole frequency range. Series resistance raised with
182 raise of gasoline concentration (Jonscher 1973, 1975, 1977 and 1999, Hill and
183 Jonscher 1983). The dry sample has very low resistance while successive
184 gasoline concentration increases the resistance sequentially. The series
185 resistance of the dry sample (0 μL) decreases with frequency increase (Garrouch
186 and Sharma 1994, Dias 2000, Chinh 2000). The variation of the series
187 resistance, nearly, takes more than one decade in the whole frequency range.
188 When specimen is contaminated with gasoline (10 μL , 20 μL , 30 μL , 40 μL , 50
189 μL and 60 μL), the resistance is higher. Resistance is raised with raise of the
190 gasoline concentration with more faster degree (with frequency), consuming
191 nearly two decades in the whole frequency range for high concentration (60
192 μL). All samples does not accomplish saturation resistance of frequency even
193 at very high frequency (2×10^7 Hz). The curves will not reach that saturation
194 resistance frequency (with frequency increase, the resistance is still decreasing,
195 Chelidze 1979, Knight and Abad 1995). Clear difference is found between the
196 series resistance value at Fig. (2) (2×10^5) for high water saturation and that
197 value of series resistance at Fig. (3) (1×10^6) for high gasoline saturation. This
198 difference is completely attached to change of the contaminant (Bussian 1983,
199 Khalafalla and Maegley 1973). The gasoline saturation is quite increases the
200 resistance and water saturation is quite decreases the resistance.

201 Fig. (4) Shows the permittivity (ϵ') with frequency dry and at various
202 concentrations of filtered water (10 μL , 20 μL , 30 μL , 40 μL , 50 μL and 60
203 μL). The successive additions of water concentrations increases the value of
204 sample permittivity by nearly one decade, at low frequency, and this value
205 decreases at relatively high frequency. At low frequency, permittivity (ϵ') has
206 relative high values that decrease with frequency increase and finally at
207 relatively high frequencies becomes independent of frequency. The the
208 permittivity decreases rapidly at relatively lower frequencies and decreases
209 slowly at relatively higher frequencies. Normal permittivity (ϵ')
210 behaviour show that there values decreases with increasing frequency until it
211 reaches a constant value. Above definite frequency range, the exchange
212 interaction of electron between the ions cannot keep track of applied electric
213 field. At relatively high frequency regions, the charge carriers would barely
214 have started to move before the field reversal occurs and the permittivity ϵ'
215 falls to its smallest values. Space charge polarization arises between grain
216 interfaces and grain-electrode interface due to inhomogeneity of permittivity
217 structure at these interfaces. This is what is called double layer; semi-
218 conducting grains separated by insulating or poor conducting grains. The
219 permittivity of a material comes from electronic, ionic and space charge
220 accumulation. The electronic contribution is the main factor that are affected by
221 the present frequency range, while at other frequency ranges other mechanisms
222 may be the dominant factors.

223 Figure (5) Shows the permittivity (ϵ') with frequency, dry and at various
224 saturations of gasoline. The successive additions of gasoline decreases the
225 value of sample permittivity by less than one decade, for lower frequency
226 ranges.

227 Figure (6) shows the complex series impedance (Z_s) for the sand-clay
228 sample dry and at various concentrations of filtered water (10 μL , 20 μL , 30
229 μL , 40 μL , 50 μL and 60 μL). For the dry condition case, measured impedance
230 shows nearly an arc (or a part of another semicircle, for lower frequencies) in
231 contact with another semicircle (at relatively higher frequency). This indicates
232 two different polarization mechanisms within the specimens. First semicircle
233 (at high frequency) shows the properties of specimen materials (bulk property).
234 The other arc or the other part of semicircle (at low frequency) shows the
235 properties of interface (grain boundary) between the grains. This may be
236 resulted from transport of charges across the grain boundaries. Complex
237 impedance was gradually decreasing with frequency increase which resulted
238 from space charge increase at relatively higher frequencies. With increase of
239 conductor concentration (distilled water), the relaxation peak proceeds to
240 higher frequency and its strength decreases. This effect that is similar in
241 behaviour, more or less, to rise of temperature.

242 Figure (7) shows the complex parallel impedance (Z_p) for the sand-clay
243 samples, dry and at various saturations of gasoline (10 μL , 20 μL , 30 μL , 40
244 μL , 50 μL and 60 μL). For dry sample, measured impedance plane shows
245 nearly an arc (at low frequency) that has low impedance than the other

246 saturated curves. This arc describes the total conductor connections at the
247 specimen. Also, we can find two different polarization mechanisms within the
248 samples (bulk at relatively higher frequency and grain boundary at relatively
249 low frequencies). As gasoline concentration increases, the impedance peaks
250 move to high values of complex impedances. Also, sequential additions of
251 gasoline concentrations cause the peaks widths to be broader and more
252 expanded. The expansion of peaks means that the barriers that the ions have to
253 overcome, due to increment of resistivity, become bigger with the additions of
254 gasoline concentrations. As insulator contaminant increases (gasoline), the
255 relaxation peak proceeds to lower frequencies and increases in its strength and
256 become broader.

257 Figure (8) displays the Nyquist representation of conductivity of sand-
258 clay with different amounts of water concentrations. Figure (8) can be
259 compared with figure (6), for impedance representation.

260 Figure (9) displays the Nyquist representation of conductivity of sand-
261 clay with different amounts of gasoline concentrations (10 μL , 20 μL , 30 μL ,
262 40 μL , 50 μL and 60 μL). The behavior of the samples in figure (9) can be
263 compared with the behavior of figure (7), for impedance representation.

264 The water contamination decreases the whole sample impedances. The
265 gasoline contamination increases the the whole sample impedances.

266

267 **3) CONCLUSION**

268 In the laboratory, conductivity of samples increases with adding water
269 concentration while with the additions of gasoline causes a conductivity to
270 decrease. Electrical conduction, in general, is raised with rise of overall
271 conductor continuous links and with frequency increase. There is a link
272 between hydrocarbons contamination and geophysical signal and the electrical
273 resistivity. The bulk conductivity observed in contaminated samples is linked
274 to contaminant fluid conductivity and its amount and consequently changes
275 according to the type of contaminant. So we could infer that type of
276 contaminant is important at altering geophysical properties of contaminated
277 sediments. Hence, influence of type of contaminant on physical properties
278 cannot be ignored in geophysical contaminated sites. Frequency effect of
279 conductivity is reflected from orientation and translation hopping. The
280 dependence of impedance on frequency indicates distribution of relaxation in
281 the samples. Imaginary impedance peaks are shifted to higher frequency side
282 with increase of filtered water. Finally, the electrical measurements are good
283 support for analysis to define qualitatively the type of contaminant.

284 **4) REFERENCES**

285 Abou El-Anwar E., Gomaa M. M., 2013, Electrical properties and
286 geochemistry of carbonate rocks from the Qasr El-Sagha formation, El-
287 Faiyum, Egypt, Geophysical Prospecting, Vol. 61, pp. 630–644.

288 Abou El-Anwar E., Gomaa M. M., 2016, Electrical, mineralogical,
289 geochemical and provenance of Cretaceous black shales, Red Sea Coast,
290 Egypt, Egyptian Journal of Petroleum, Vol. 25, pp. 323- 332.

291 Barabanova E V, Malyshkina O V, Ivanova A I, Posadova E M,
292 Zaborovskiy K M and Daineko A V, Effect of porosity on the electrical
293 properties of PZT ceramics., *Materials Science and Engineering* 49 (2013)
294 012026 doi:10.1088/1757-899X/49/1/012026

295 Bussian A. E., 1983, Electrical conductance in a porous medium,
296 *Geophys.*, Vol. 48, No. 9, pp. 1258- 1268.

297 Chelidze T. and Guéguen Y., 1999, Electrical spectroscopy of porous
298 rocks: a review -I. Theoretical models, *Geophys. J. Int.*, 137, 1–15.

299 Chelidze T. Guéguen Y. and Ruffet C., 1999, Electrical spectroscopy of
300 porous rocks: a review -II. Experimental results and interpretation, *Geophys. J.*
301 *Int.*, 137, 16-34.

302 Chelidze T. L., 1979, A Percolation model of the electrical conductivity of
303 minerals, *Izvestiya, Earth Physics*, Vol. 15, No. 11.pp. 849- 850.

304 Chew W. C., and Sen P. N., 1982, Dielectric enhancement due to
305 electrochemical double layer: thin double layer approximation, *J. Chem. Phys.*,
306 Vol. 77, No. 9, pp. 4683- 4693.

307 Chinh P. D., 2000, Electrical properties of sedentary rocks having
308 interconnected water- saturated pore spaces, *Geophysics*, Vol. 65, No. 4, pp.
309 1093- 1097.

310 Dias C. A., 2000, Development in a model to describe low- frequency
311 electrical polarization of rocks, *Geophys.*, Vol. 65, No. 2, pp. 437- 451.

312 Garrouch A. A. and Sharma M. M., 1994, The influence of clay content,
313 Salinity, Stress, and wettability on the dielectric properties of brine- saturated
314 rocks: 10 Hz to 10 MHz, *Geophys.*, Vol. 59, No. 6, pp. 909- 917.

315 Gomaa M. M., 2008, Relation between electric properties and water
316 saturation for hematitic sandstone with frequency, *Annals of Geophysics*, Vol.
317 51, No. 5/6, pp. 801-811.

318 Gomaa M. M., 2009, Saturation effect on Electrical properties of hematitic
319 sandstone in the audio frequency range using non-polarizing electrodes,
320 *Geophysical Prospecting*, Vol. 57, pp. 1091–1100.

321 Gomaa M. M., 2013, Forward and inverse modeling of the electrical
322 properties of magnetite intruded by magma, Egypt, *Geophysical Journal*
323 *International*, Vol. 194, Issue 3, pp. 1527-1540.

324 Gomaa M. M., Abou El-Anwar E., 2015, Electrical and geochemical
325 properties of tufa deposits as related to mineral composition in South Western
326 Desert, Egypt, *Journal of Geophysics and Engineering*, Vol. 12, No. 3, pp. 292-
327 302.

328 Gomaa M. M., Abou El-Anwar E., 2017, Electrical, mineralogical, and
329 geochemical properties of Um Gheig and Um Bogma Formations, Egypt,
330 *Carbonates and Evaporites*, pp. 1-14.

331 Gomaa M. M., Alikaj P., 2009, Effect of electrode contact impedance on a.
332 c. electrical properties of wet hematite sample, *Marine Geophysical researches*,
333 Volume 30, Number 4, pp. 265-276.

334 Gomaa M. M., Elsayed R. M., 2006, Thermal Effect of Magma Intrusion
335 on Electrical Properties of Magnetic Rocks from Hamamat Sediments, NE
336 Desert, Egypt, presented at the 68th Conference and Exhibition incorporating
337 SPE Europe: European Association of Geoscientists and Engineers (EAGE),
338 Poster P328, Session " Gravity, Magnetism, Mining and Geothermal ",
339 Opportunities in Mature Areas 6, 12- 15 June, Vienna, Austria, pp. 3550-3555.

340 Gomaa M. M., Elsayed R. M., 2009, Thermal Effect of Magma Intrusion
341 on Electrical Properties of Magnetic Rocks from Hamamat Sediments, NE
342 Desert, Egypt, Geophysical Prospecting, Vol. 57, No. 1, pp. 141-149.

343 Gomaa M. M., Hussain S. A., El- Diwany E. A., Bayoumi A. E., and
344 Ghobashy M. M., 2000, Modeling of A. C. electrical properties of humid sand
345 and the effect of water content, Society of Exploration Geophysicists (SEG),
346 International Exposition and 70th Annual Meeting, Calgary, Alberta, Canada,
347 19 (1), pp. 1850-1853.

348 Gomaa M. M., Kassab M., 2016, Pseudo random renormalization group
349 forward and inverse modeling of the electrical properties of some carbonate
350 rocks, Journal of Applied Geophysics, Vol. 135, pp. 144- 154.

351 Gomaa M. M., Kassab M., 2017, Forward and inverse modelling of
352 electrical properties of some sandstone rocks using renormalisation group
353 method, Near Surface Geophysics, Vol. 15 (5), pp. 487- 498.

354 Gomaa M. M., Kassab M., El-Sayed N. A., 2015 a, Study of petrographical
355 and electrical properties of some Jurassic carbonate rocks, north Sinai, Egypt,
356 Egyptian Journal of Petroleum, Vol. 24 (3), pp. 343- 352.

357 Gomaa M. M., Kassab M., El-Sayed N. A., 2015 b, Study of electrical
358 properties and petrography for carbonate rocks in the Jurassic Formations:
359 Sinai Peninsula, Egypt, Arabian Journal of Geosciences, Vol. 8, Issue 7, pp.
360 4627-4639.

361 Gomaa M. M., Metwally H., Melegy A., 2018, Effect of concentration of
362 salts on electrical properties of sediments, Lake Quaroun, Fayium, Egypt,
363 Carbonates and Evaporites, pp. 1-9.

364 Gomaa M. M., Shaltout A., Boshta M., 2009, Electrical properties and
365 mineralogical investigation of Egyptian iron ore deposits, Materials Chemistry
366 and Physics, Volume 114, Issue 1, 2009, pp. 313-318.

367 Gomaa M.M., 2006, Interpretation of Electrical Properties for Humid and
368 Saturated Hematitic Sandstone Sample, presented at the 68th Conference and
369 Exhibition incorporating SPE Europe: European Association of Geoscientists
370 and Engineers (EAGE), Oral H021, Session "Gravity, Magnetics, Mining and
371 Geothermal", Opportunities in Mature Areas 4, 12- 15 June, Vienna, Austria,
372 pp. 2182-2186.

373 Hill R. M. and Jonscher A. K., 1983, The dielectric behavior of condensed
374 matter and its many- body interpretation, Contemp. Phys., Vol. 24, No. 1, pp.
375 75- 110.

376 Jonscher A. K., 1973, Carrier and matrix losses in solid dielectrics, In 1972
377 Annual report conference on Electrical insulation and dielectric phenomena,
378 (Natn: Academy of Sci., Washington D. C., 1973), pp. 418- 425.

379 Jonscher A. K., 1975, The interpretation of non- dielectric admittance and
380 impedance diagrams, Phys. Stat. Sol. (a) 32, pp. 665- 675.

381 Jonscher A. K., 1977, Review article the universal dielectric response,
382 Nature, Vol. 267, pp. 673- 679.

383 Jonscher A. K., 1999, Review article Dielectric relaxation in solids, J.
384 Phys. D: Appl. Phys., Vol. 32, pp. R57- R70.

385 Kassab M., Gomaa M. M., Lala A., 2017, Relationships between electrical
386 properties and petrography of El-Maghara sandstone formations, Egypt,
387 NRIAG Journal of Astronomy and Geophysics, Vol. 6, pp.162-173.

388 Khalafalla A. S. and Maegley W. J., 1973, Low- frequency impedance
389 parameters of basalt, Granite, and Quartzite, Geophys., Vol. 38, No. 1, pp. 68-
390 75.

391 Knight R. J. and Abad A., 1995, Rock/ water interaction in dielectric
392 properties: Experiments with Hydrophobic sandstones, Geophys., Vol. 60, No.
393 2, pp. 431- 436.

394 Knight R. J. and Nur A., 1987, The permittivity of sandstones, 60 kHz to 4
395 MHz, Geophys., pp. 644- 654.

396 Last B. J., and Thouless D. J., 1971, Percolation theory and electrical
397 conductivity, Phys. Rev. Lett., Vol. 27, No. 25, pp. 1719- 1721.

398 Leroy P., Revil A., Kemna A., Cosenza P. and Ghorbani A., 2008,
399 Complex conductivity of water-saturated packs of glass beads, Journal of
400 Colloid and Interface Science, Volume 321, Issue 1, pp. 103-117

401 Levitskaya T. M., 1984, Dielectrical relaxation in rock, *Izvestiya, Earth*
402 *physics*, Vol. 20, No. 10, pp. 777- 780.

403 Levitskaya T. M., Sternberg B. K., 1996 a, Polarization processes in rocks
404 1. Complex dielectric permittivity method, *Radio Science*, vol. 31, No. 4, pp.
405 755- 779.

406 Levitskaya T. M., Sternberg B. K., 1996 b, Polarization processes in rocks
407 2. Complex dielectric permittivity method, *Radio Science*, vol. 31, No. 4, pp.
408 781- 802.

409 Mendelson K. S., and Cohen M. H., 1982, The effect of grain anisotropy
410 on the electrical properties of sedimentary rocks, *Geophys.*, Vol. 47, No. 2, pp.
411 257- 263.

412 Minaw F., Hanna B., Mikhail F. N., 1972, Relation between the
413 permittivity and the dielectric loss for some Egyptian rocks, *Egypt. J. Geol.*,
414 Vol. 16, No. 2, pp. 293- 301.

415 Olhoeft G. R., 1976, electrical properties of rocks, in the physics and
416 chemistry of minerals and rocks, R. G. J. Sterns, ed., Wiley, NY. pp. 261-278.

417 Olhoeft G. R., 1977, Electrical properties of natural clay permafrost, *Can.*
418 *J. Earth Sci.*, Vol. 14, pp. 16- 24.

419 Olhoeft G. R., 1980, Electrical properties of rocks: in *Physical properties of*
420 *rocks and minerals*: Touloukian Y. S., Judd W. R., & Roy R. F., Eds.,
421 McGraw- Hill Book Co., 257-330.

422 Olhoeft G. R., 1985, low- frequency electrical properties, *Geophys.*, Vol.
423 50, No. 12, pp. 2492- 2503.

424 Sen P. N., 1981, Dielectric anomaly in inhomogeneous materials with
425 application to sedimentary rocks, *Appl. Phys. Lett.*, Vol. 39, No. 8, pp. 667-
426 668.

427 Sen P. N., 1984, Short note: Grain shape effects on dielectric and electrical
428 properties of rocks, *Geophys.*, Vol. 49, No. 5, pp. 586- 587.

429 Shaltout A. A., Gomaa M. M., Wahbe M., 2012, Utilization of standardless
430 analysis algorithms using WDXRF and XRD for Egyptian Iron Ores
431 identification, *X-Ray Spectrometry*, Vol. 41, pp. 355–362.

432 Song Y., Noh T. W., Lee S., & Gaines R., 1986, Experimental study of the
433 three- dimensional ac Conductivity and permittivity of a conductor- insulator
434 composite near the percolation threshold, *Phys. Rev. B*, Vol. 33, No. 2, pp.
435 904- 908.

436

437

Table Caption

438 Table (1) Chemical analysis, Particle size analysis, Hydrogeological properties
439 (d_m : average diameter; K_{max} : hydraulic permeability; r : porosity).

440

Figure Caption

441 Fig (1) Displaying sample cell, where 1 is a Teflon cylinder a 2 are the two
442 electrodes enclosing the sample.

443 Fig. (2) Shows the series resistance (R_s) as a function of frequency dry and at
444 different saturations of distilled water.

445 Fig. (3) Shows the series resistance (R_s) as a function of frequency dry and at
446 different saturations of gasoline.

447 Fig. (4) Shows the permittivity (ϵ') as a function of frequency dry and at
448 different saturations of distilled water.

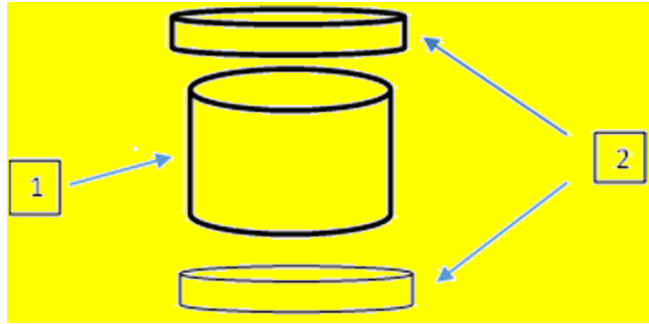
449 Fig. (5) Shows the permittivity (ϵ') as a function of frequency dry and at
450 different saturations of gasoline.

451 Fig. (6) Shows the complex series impedance (Z_s) for the sand-clay sample dry
452 and at different saturations of distilled water.

453 Fig. (7) Encloses the complex series impedance (Z_p) for the sand-clay sample
454 dry and at different saturations of gasoline.

455 Fig. (8) displays the Nyquist plot of the conductivity of sand-clay as a function
456 of different amounts of water.

457 Fig. (9) displays the Nyquist plot of the conductivity of sand-clay as a function
458 of different amounts of Gasoline.



459

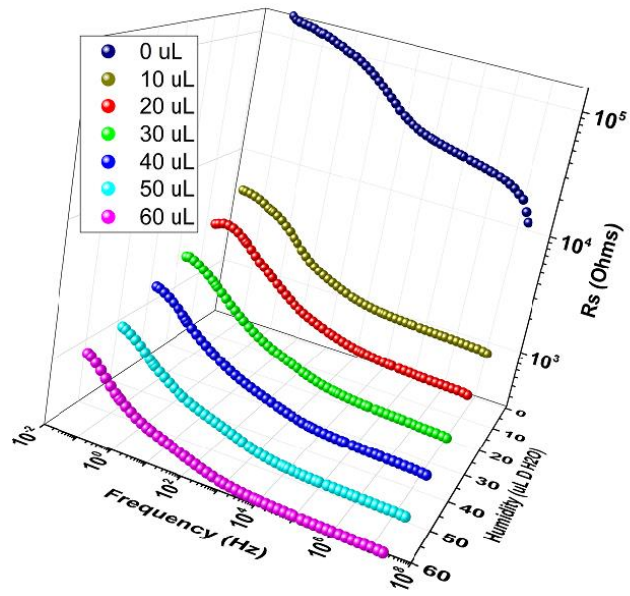
460

Fig. (1) Show sample cell holder, 1) is the Teflon cylinder and 2) two

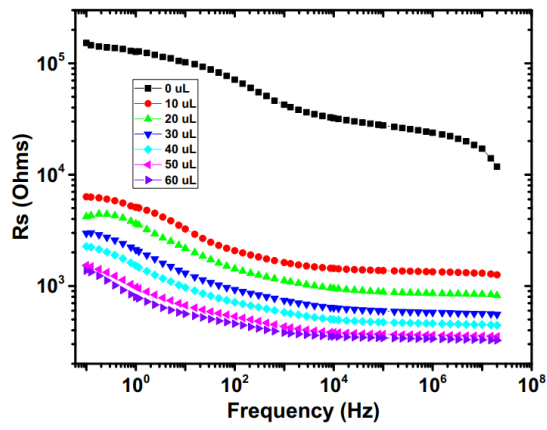
461

electrodes enclosing the sample.

462



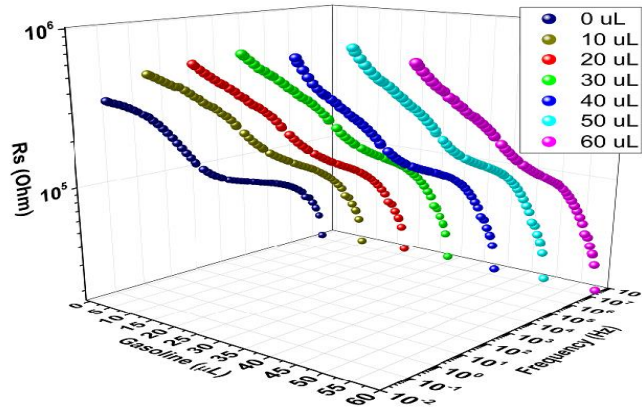
463



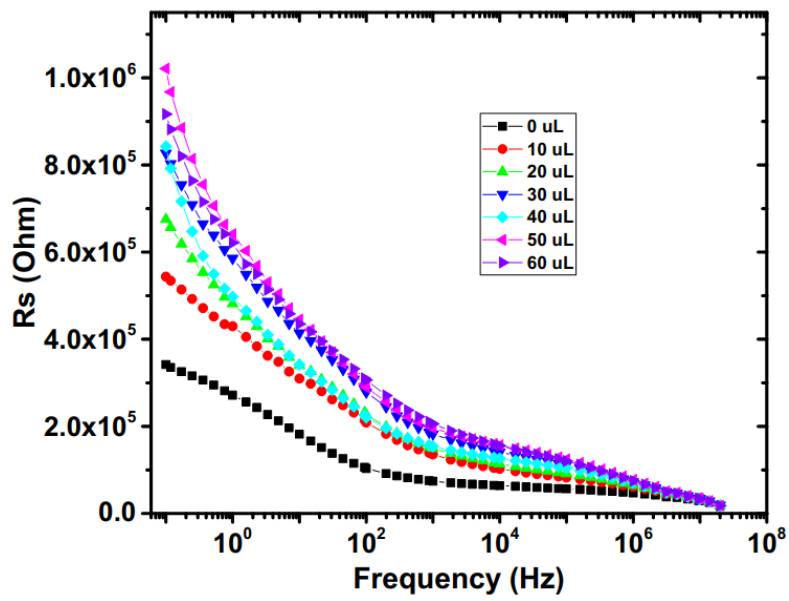
464

465 Fig. (2) Shows the series resistance (R_s) with frequency, dry and at various
 466 saturations of distilled water.

467



468



469

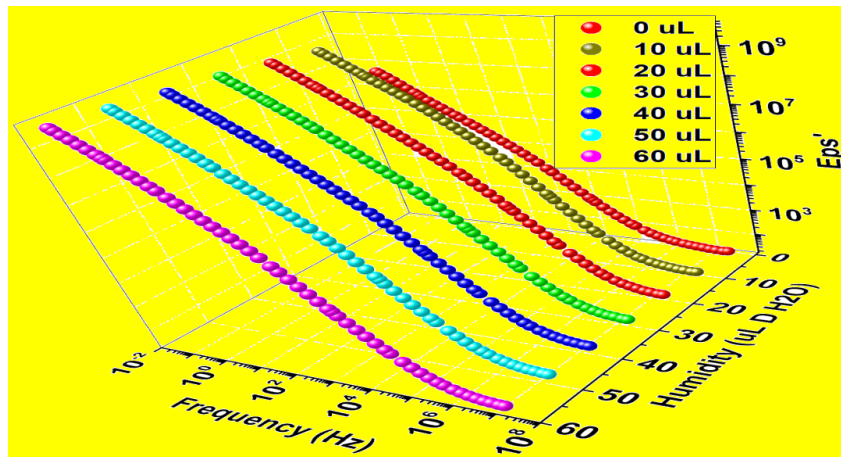
470 Fig. (3) Shows the series resistance (R_s) with frequency, dry and at various

471

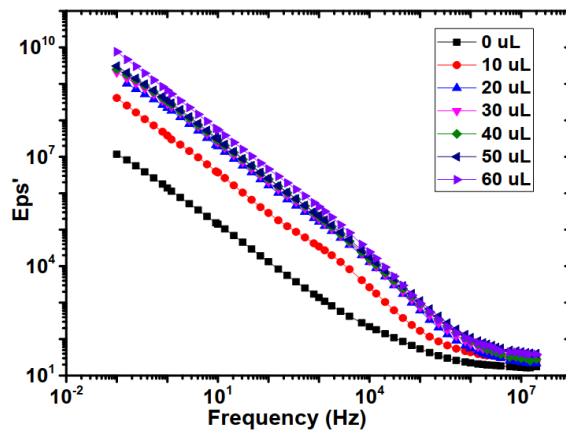
saturation of gasoline.

472

473



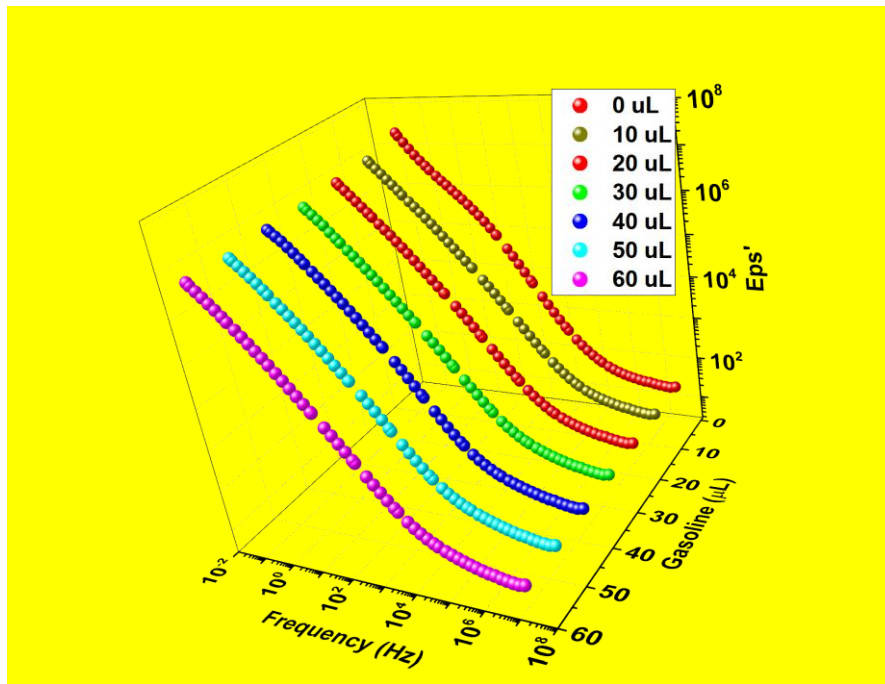
474



475

476 Fig. (4) Shows the permittivity (ϵ') with frequency, dry and at various
477 saturations of distilled water.

478



480

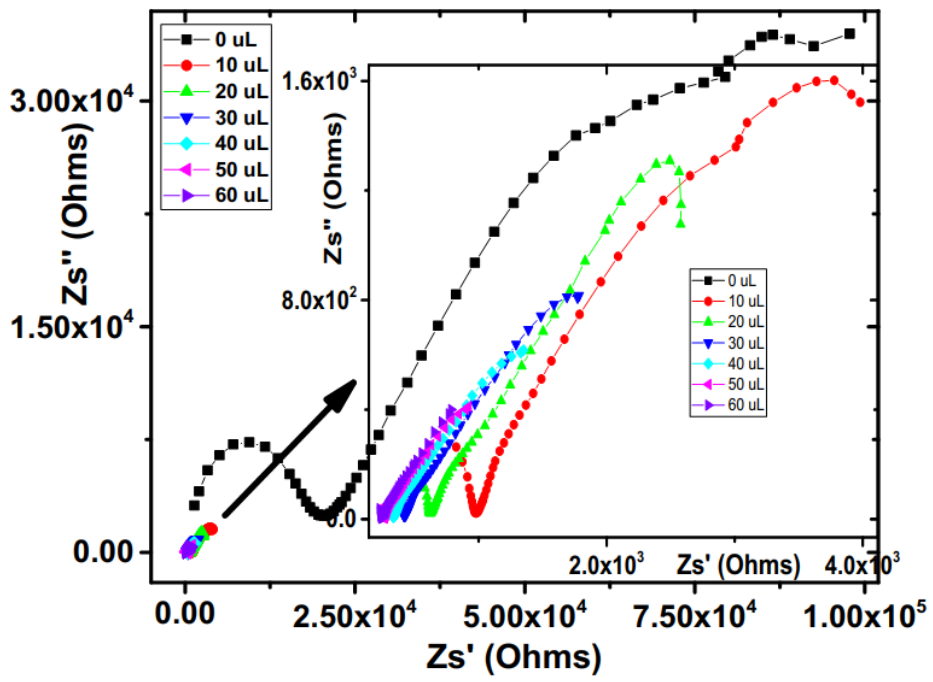
481 Fig. (5) Shows the permittivity (ϵ') with frequency, dry and at various

482

saturations of gasoline.

483

484



485

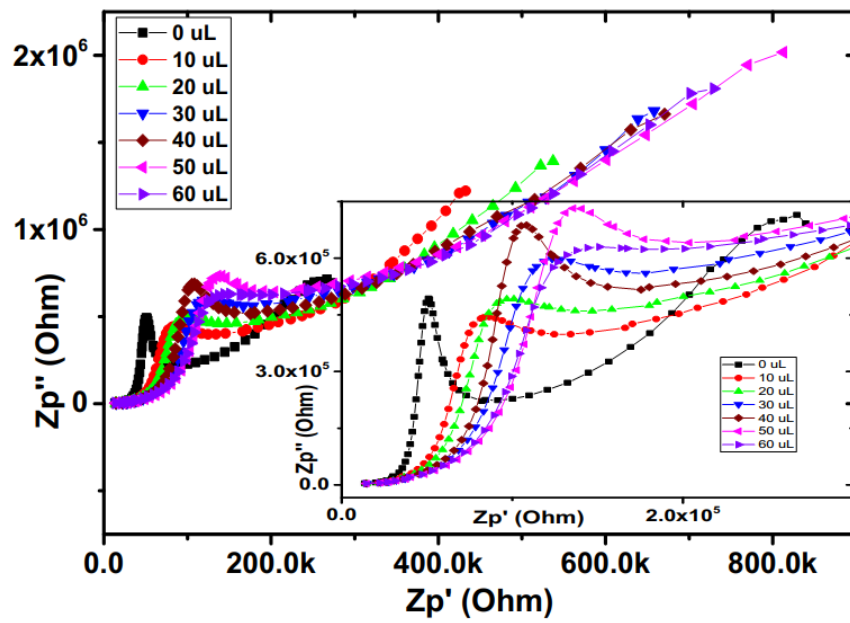
486

Fig. (6) Shows the complex series impedance (Z_s) for the sand-clay

487

sample dry and at various saturations of filtered water.

488



490

491

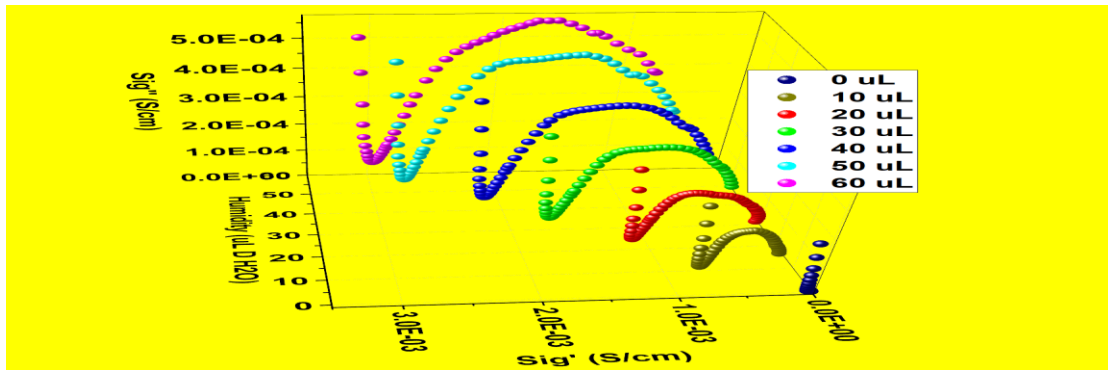
Fig. (7) Encloses the complex series impedance (Z_p) for the sand-clay

492

sample dry and at various saturations of gasoline.

493

494



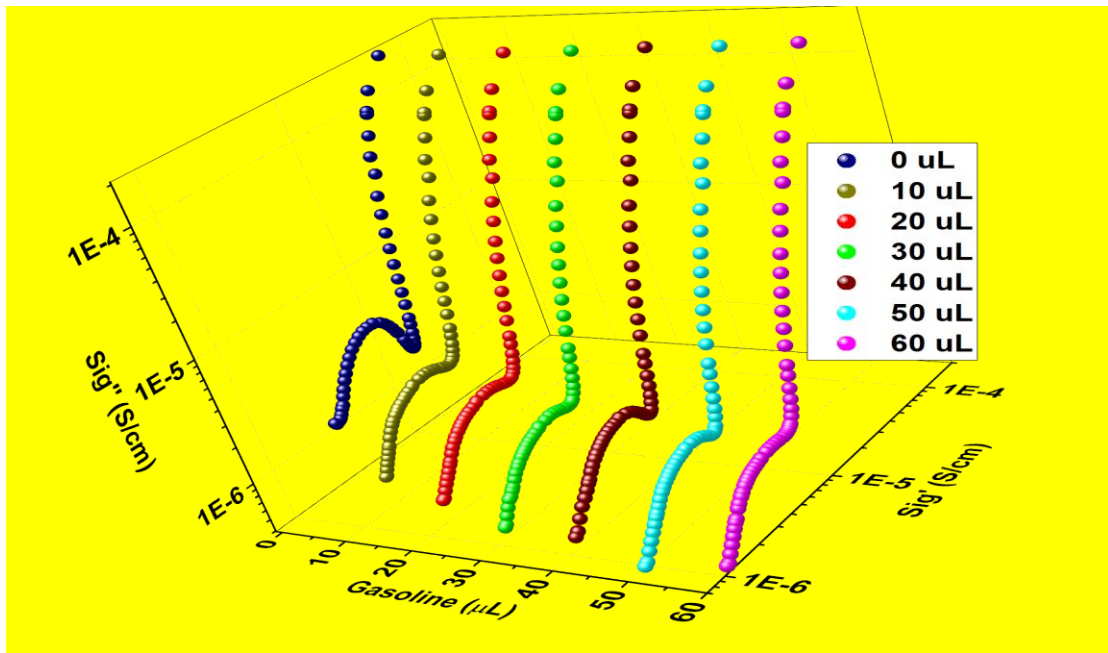
495

496 Fig. (8) displays the Nyquist representation of conductivity of sand-clay with

497

different amounts of water.

498



500

501 Fig. (9) displays the Nyquist representation of conductivity of sand-clay with

502 different amounts of gasoline concentrations.

503